

Panchromatic Views of Large-scale Extragalactic Jets

C. C. Cheung¹

Kavli Institute for Particle Astrophysics and Cosmology
Stanford University, Stanford, CA 94305, USA

Abstract. Highlights of recent observations of extended jets in AGN are presented. Specifically, we discuss new spectral constraints enabled by *Spitzer*, studies of the highest-redshift ($z\sim 4$) radio/X-ray quasar jets, and a new *VLBA* detection of superluminal motion in the M87 jet associated with a recent dramatic X-ray outburst. Expanding on the title, inverse Compton emission from extended radio lobes is considered and a testable prediction for the gamma-ray emission in one exemplary example is presented. Prospects for future studies with *ALMA* and low-frequency radio interferometers are briefly described.

1. Shedding New Light on Large-scale Extragalactic Jets

Chandra observations have established that X-ray emission is a common feature of radio jets in active galactic nuclei (AGN) on kiloparsec scales. Harris & Krawczynski (2006, and the accompanying website²) provided an extensive recent review of this topic. Here, we focus on some of the more recent observational results reported subsequent to this review.

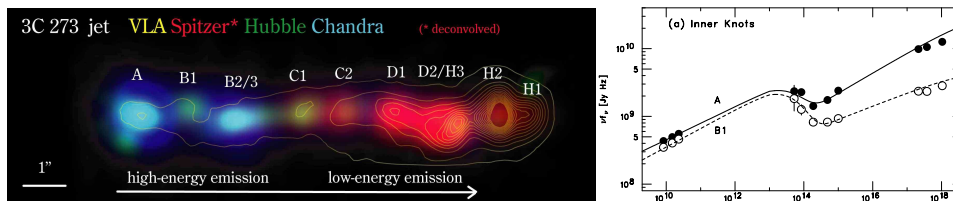


Figure 1. Multi-band arcsec-resolution image of the 3C 273 jet and sample knot SEDs (from Uchiyama et al. 2006).

Multi-wavelength studies of radio jets have relied on the sub-arcsecond resolution imaging capabilities of *Hubble* and *Chandra*; additional spectral constraints are now being obtained with *Spitzer*. Recent mid-IR detections of the 3C 273 jet (Uchiyama et al. 2006) and the hotspots in Cygnus A (L. Stawarz et al., in preparation) have clarified the relationship between the X-ray and lower-energy emission. Specifically in 3C 273, most of the optical/UV emission

¹Jansky Postdoctoral Fellow of the National Radio Astronomy Observatory. The NRAO is operated by Associated Universities, Inc. under a cooperative agreement with the NSF.

²<http://hea-www.harvard.edu/XJET/> lists 78 X-ray jet and hotspot detections as of Dec 2006.

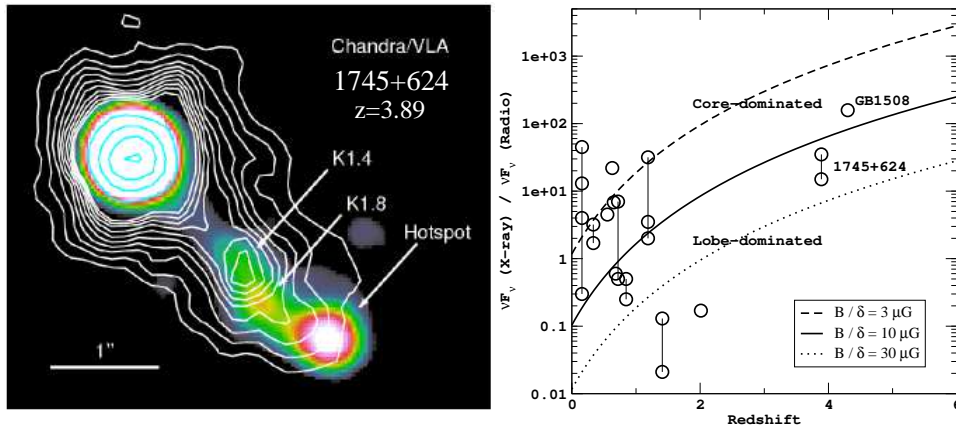


Figure 2. [left] The X-ray (contours) and radio (color) jet in the $z=3.9$ quasar 1745+624 (from Cheung et al. 2006; $1''=7.2$ kpc). [right] Plot of observed f_x/f_r vs. redshift for X-ray jets in quasars (adapted from Cheung 2004, with the addition of the 1745+624 case). Vertical lines connect different knots from the same jet. Curves indicate expected f_x/f_r ratio for the given combinations of B and δ (for $\alpha=1$), which in the IC/CMB model, scale as $(1+z)^4$. The central solid curve approximately separates knots in core-dominated (larger δ) and lobe-dominated (smaller δ) sources.

($\sim 10^{15}$ Hz) in the inner jet knots lie essentially on a power-law extrapolation of the X-rays (Fig. 1), providing definition of this high-energy spectral component. Since the jet is long known to be optically polarized, an indelible signature of synchrotron radiation, it is reasonable to infer a synchrotron origin for the X-rays also. The significance of this result to the wider applicability of synchrotron and inverse Compton (IC off the CMB) models in other X-ray jets is so far not clear since this spectral signature has not been defined so clearly in any other extragalactic jet. New *Spitzer* observations of 10 other powerful X-ray/radio jets selected from XJET² are being obtained (PI: Y. Uchiyama) and optical/UV polarization imaging will be useful in this respect.

One potentially distinguishing feature between synchrotron and IC/CMB models is that the latter predicts high- z quasars to have bright X-ray jets because of the strong z -dependence of the CMB energy density. Specifically, we expect an observed monochromatic X-ray to radio flux ($f_\nu \equiv \nu F_\nu$) ratio, $f_x/f_r \simeq u_{\text{cmb}}/u_B \simeq 10(1+z)^4 \delta^2 / B_{\mu\text{G}}^2$ if IC emission dominates (δ is the relativistic Doppler factor and $\alpha=1$ is assumed), whereas we expect $f_x/f_r \propto z^0$ in the synchrotron case. Two very high-redshift ($z \sim 4$) jets are currently clearly detected in both X-ray and radio bands (Cheung, Stawarz, & Siemiginowska 2006, and refs. therein). The observed f_x/f_r ratio of these jets are systematically larger than in lower- z examples (Fig. 2), as one expects in the IC/CMB scenario. Differences in B and jet δ then accounts for the widely varying f_x/f_r ratios in different jets at similar redshifts; this picture makes clear predictions for jets aligned away from our line of sight, i.e., lobe-dominated quasars. *Chandra* observations of four additional $z \sim 4-5$ quasars with known arcsec-scale radio jets being obtained in the current cycle will shed further light on this issue.

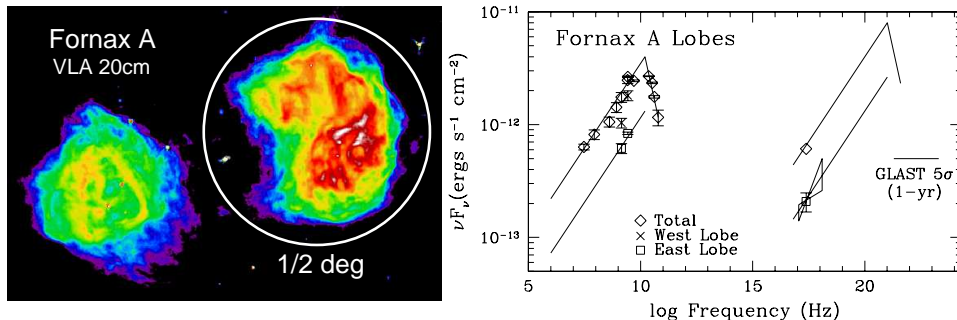


Figure 3. Radio image of the double-lobed radio galaxy Fornax A (data from Fomalont et al. 1989) and SEDs of its different components. At a distance of 18.6 Mpc, the 0.5° diameter circle corresponds to 162 kpc. The low-frequency radio data were compiled by Isobe et al. (2006; Fig. 5 therein) with additional 23–61 GHz data from *WMAP* (the 94 GHz measurement is omitted because of its lower significance). The predicted IC/CMB components assume $B=1.5\mu\text{G}$ in the lobes to match the detected X-rays.

One last highlight comes courtesy of the well-known jet in M87. The X-ray and optical intensities of the knot HST-1 in the jet (~ 60 pc projected from the nucleus) had been continually increasing since 2000, reaching a maximum in early 2005 ($\times 50$ increase; Harris et al. 2006). New *VLBA* observations were obtained when HST-1 became bright enough in the radio and revealed several superluminal ($1.4\text{--}4c$) ejections associated with the onset of activity. The recent *HESS* report of a TeV flare (Aharonian et al. 2006) broadly mimicking the *VLA/HST/Chandra* lightcurves of HST-1 give us unique insight into flares in more distant blazars (C.C. Cheung & D.E. Harris, in preparation). Monitoring is being continued and we expect to extend this program into the *GLAST* era.

2. Compton X-ray to Gamma-ray Emission in Radio Lobes

Since the CMB is ubiquitous, IC/CMB losses are mandatory in synchrotron sources. This emission is most prominent in regions of low magnetic field like the extended lobes of radio galaxies, and many such sources of IC/CMB X-rays are now known (e.g., Croston et al. 2005; Kataoka & Stawarz 2005). Perhaps one of the best examples of IC/CMB X-rays is in the nearby radio galaxy Fornax A (Feigelson et al. 1995) which we further discuss as an exemplary example.

Fornax A is a bright nearby radio galaxy and integrated radio measurements extend down to ~ 30 MHz (Isobe et al. 2006). It is detected out to ~ 90 GHz by *WMAP* (Fig. 3) with a steep cm-wave spectrum, $F_\nu \propto \nu^{-1.5 \pm 0.09}$ (Bennett et al. 2003). Ignoring kinematic factors, we can relate the synchrotron to IC/CMB spectra by $\nu_{\text{synch}}[\text{MHz}] \sim 2E_{\text{IC}}[\text{keV}]B_{\mu\text{G}}/(1+z)$, and figure 3 shows the predicted IC component for Fornax A. This assumes an average $B=1.5\mu\text{G}$ in the lobes to match the X-ray detections (Feigelson et al. 1995; Isobe et al. 2006). The expectation is that the electrons producing radio emission in the observed $\sim 10^8\text{--}10^{10}$ GHz range will produce a hard X-ray/soft γ -ray emission signal. Sub-mm observations can show the extent of this extrapolation in the *GLAST* sensitivity

range. Fornax A is quite extended in the sky, so if it is detected by *GLAST*, the contributions from the two lobes will be separable.

3. Observational Prospects

Detailed resolved spectral studies utilizing *Chandra*, *Spitzer*, and *Hubble*, are currently limited mainly to the brightest jets and hotspots. In the future, *JWST* may detect fainter examples and *ALMA* will “catch” those with spectral cut-offs in the ~ 10 's to ~ 1000 GHz range to better define their synchrotron continua. Another course of study enabled by *ALMA* is to search for the signature of “bulk-Compton” emission from a relativistic stream of cold particles (i.e., $\langle \gamma \rangle \sim 1$) scattering the CMB. In Uchiyama et al. (2005), our non-detection of this “bump” in the mid-IR argues against a pure e^+e^- jet in quasar PKS 0637 if $\Gamma \sim 10$ –15 as required by an IC/CMB origin for the X-rays. If instead, jets like this are only mildly relativistic ($\Gamma \sim 2$ –3), the bulk Compton bump then peaks at $\nu \sim \Gamma^2 \nu_{\text{cmb}} \sim 160\Gamma^2(1+z)$ GHz which is near the *ALMA* sensitivity range; such observations can then test emission models.

The next generation of low radio frequency interferometers like the *Long Wavelength Array (LWA)* will provide radio maps with unprecedented sensitivity and resolution at 10's–100's MHz. These observations will measure synchrotron emission from the low-energies electrons which are responsible for IC emission in the UV/X-ray bands (see Harris 2005 for such applications). In the example of Fornax A (§2.), the first prototype antenna tiles of the *Mileura Widefield Array (MWA)* Low-Frequency Demonstrator already show the double-structure at ~ 100 MHz (Bowman et al. 2006) that is known at higher-frequencies. We can look forward to detailed maps of the various components of even fainter, more distant radio sources as construction of the arrays progresses. If the emission extends into the cm–mm range in regions of relatively low magnetic field ($\sim \text{few } \mu\text{G}$), it will signal IC/CMB emission in the hard X-ray/soft γ -ray bands as postulated in the case of Fornax A; some of the brightest examples should be detectable and image-able with *GLAST*.

References

- Aharonian, F., et al. (H.E.S.S. collaboration) 2006, *Science*, 314, 1424
 Bennett, C.L., et al. 2003, *ApJS*, 148, 97
 Bowman, J.D., et al. 2006, *AJ*, in press (astro-ph/0611751)
 Cheung, C.C. 2004, *ApJL*, 600, L23
 Cheung, C.C., Stawarz, L., & Siemiginowska, A. 2006, *ApJ*, 650, 679
 Croston, J. H., et al. 2005, *ApJ*, 626, 733
 Feigelson, E.D., et al. 1995, *ApJ*, 449, L149
 Fomalont, E.B., et al. 1989, *ApJ*, 346, L17
 Harris, D.E. 2005, ASP Conf. Ser. 345, N.E. Kassim et al. eds., 254
 Harris, D.E., et al. 2006, *ApJ*, 640, 211
 Harris, D.E., & Krawczynski, H. 2006, *ARA&A*, 44, 463
 Isobe, N., et al. 2006, *ApJ*, 645, 256
 Kataoka, J., & Stawarz, L. 2005, *ApJ*, 622, 797
 Uchiyama, Y., et al. 2005, *ApJL*, 631, L113
 Uchiyama, Y., et al. 2006, *ApJ*, 648, 910